

# The TeV spectrum of H 1426+428

D. Petry<sup>1</sup>, I.H. Bond<sup>2</sup>, S.M. Bradbury<sup>2</sup>, J.H. Buckley<sup>3</sup>, D.A. Carter-Lewis<sup>1</sup>, W. Cui<sup>4</sup>, C. Duke<sup>5</sup>, I. de la Calle Perez<sup>2</sup>, A. Falcone<sup>4</sup>, D.J. Fegan<sup>6</sup>, S.J. Fegan<sup>7,15</sup>, J.P. Finley<sup>4</sup>, J.A. Gaidos<sup>4</sup>, K. Gibbs<sup>7</sup>, S. Gammell<sup>6</sup>, J. Hall<sup>9</sup>, T.A. Hall<sup>1,16</sup>, A.M. Hillas<sup>2</sup>, J. Holder<sup>2</sup>, D. Horan<sup>7</sup>, M. Jordan<sup>3</sup>, M. Kertzman<sup>8</sup>, D. Kieda<sup>9</sup>, J. Kildea<sup>6</sup>, J. Knapp<sup>2</sup>, K. Kosack<sup>3</sup>, F. Krennrich<sup>1</sup>, S. LeBohec<sup>1</sup>, P. Moriarty<sup>10</sup>, D. Müller<sup>10</sup>, T.N. Nagai<sup>9</sup>, R. Ong<sup>11</sup>, M. Page<sup>5</sup>, R. Pallassini<sup>2</sup>, B. Power-Mooney<sup>6</sup>, J. Quinn<sup>6</sup>, N.W. Reay<sup>12</sup>, P.T. Reynolds<sup>13</sup>, H.J. Rose<sup>2</sup>, M. Schroedter<sup>7,15</sup>, G.H. Sembroski<sup>4</sup>, R. Sidwell<sup>12</sup>, N. Stanton<sup>12</sup>, S.P. Swordy<sup>14</sup>, V.V. Vassiliev<sup>9</sup>, S.P. Wakely<sup>14</sup>, G. Walker<sup>9</sup>, T.C. Weekes<sup>7</sup>

## ABSTRACT

The BL Lac object H1426+428 was recently detected as a high energy  $\gamma$ -ray source by the VERITAS collaboration (Horan et al. 2002). We have reanalyzed the 2001 portion of the data used in the detection in order to examine the spectrum of H1426+428 above 250 GeV. We find that the time-averaged spectrum agrees with a power law of the shape

$$\left(\frac{dF}{dE}\right)(E) = 10^{-7.31 \pm 0.15_{\text{stat}} \pm 0.16_{\text{sys}}} \cdot E^{-3.50 \pm 0.35_{\text{stat}} \pm 0.05_{\text{sys}}} \text{ m}^{-2} \text{ s}^{-1} \text{ TeV}^{-1}$$

The statistical evidence from our data for emission above 2.5 TeV is  $2.6 \sigma$ . With 95% c.l., the integral flux of H1426+428 above 2.5 TeV is larger than 3% of the corresponding flux from the Crab Nebula. The spectrum is consistent with the (non-contemporaneous) measurement by Aharonian et al. (2002) both in shape and in normalization. Below 800 GeV, the data clearly favours a spectrum steeper than that of any other TeV Blazar observed so far indicating a difference in the processes involved either at the source or in the intervening space.

*Subject headings:* BL Lacertae objects: individual (H 1426+428) —  $\gamma$  rays: observations

---

<sup>1</sup>Department of Physics and Astronomy, Iowa State University, Ames, IA 50011

<sup>2</sup>Department of Physics, University of Leeds, Leeds, LS2 9JT, Yorkshire, England, UK

<sup>3</sup>Department of Physics, Washington University, St. Louis, MO 63130

<sup>4</sup>Department of Physics, Purdue University, West Lafayette, IN 47907

<sup>5</sup>Physics Department, Grinnell College, Grinnell, IA 50112

<sup>6</sup>Physics Department, National University of Ireland, Belfield, Dublin 4, Ireland

<sup>7</sup>Fred Lawrence Whipple Observatory, Harvard-Smithsonian CfA, Amado, AZ 85645

<sup>8</sup>Physics Department, De Pauw University, Greencastle, IN, 46135

<sup>9</sup>High Energy Astrophysics Institute, University of Utah, Salt Lake City, UT 84112

<sup>10</sup>School of Science, Galway-Mayo Institute of Technology, Galway, Ireland

<sup>11</sup>Department of Physics, University of California, Los Angeles,

## 1. Introduction

The BL Lac object H1426+428 was discovered at optical wavelengths with a redshift of 0.129 by Remillard et al. (1989). Measurements of the spectral energy distribution of this close object are still sparse and do not sufficiently cover the expected broad two-peak

---

CA 90095

<sup>12</sup>Department of Physics, Kansas State University, Manhattan, KS 66506

<sup>13</sup>Department of Physics, Cork Institute of Technology, Cork, Ireland

<sup>14</sup>Enrico Fermi Institute, University of Chicago, Chicago, IL 60637

<sup>15</sup>Department of Physics, University of Arizona, Tucson, AZ 85721

<sup>16</sup>Department of Physics and Astronomy, University of Arkansas, Little Rock, AR 72204

structure that is familiar from other BL Lac objects (see, e.g., Donato et al. (2001)). The first peak is expected at X-ray energies and is thought to represent the synchrotron emission from relativistic electrons in the source. The second peak is expected at  $\gamma$ -ray energies and is explained in so-called leptonic models as stemming from low-energy photons which are inverse-Compton scattered to  $\gamma$ -ray energies by the same population of relativistic electrons that causes the synchrotron radiation. Alternative models attribute the second peak and also part of the X-ray emission to processes involving protons which are co-accelerated with the X-ray-emitting electrons or even partially produce them. For recent reviews see, e.g., Ghisellini (2000), Rachen (2000), Sikora & Madejski (2000).

A lower limit on the position of the X-ray peak of H1426+428 was placed by Costamante et al. (2001) at 100 keV. Currently the only published measurements above 100 keV come from Cherenkov telescopes above 280 GeV (Horan et al. 2002) and above 700 GeV (Aharonian et al. 2002). Costamante & Ghisellini (2002) predict the peak of the  $\gamma$ -ray emission of H1426+428 to be at several ten GeV.

The study of the high-energy spectrum of this “new” TeV source is especially interesting since its redshift is four times as large as that of Mkn 421 and Mkn 501, the only other extragalactic objects detected at TeV energies with good spectral information. Due to this larger distance, it is expected that signs of absorption of the  $\gamma$ -radiation via interaction with the intergalactic optical and infra-red background (IIRB) will be more pronounced, possibly permitting one to infer constraints on the IIRB photon density.

In this letter, we present the results of a spectral reanalysis of H1426+428 observations made with the Whipple 10 meter  $\gamma$ -ray telescope on Mt. Hopkins, Arizona, in the first half of 2001. We use our standard method described in Mohanty et al. (1998) for deriving the spectrum. Due to the weakness of the source and the special interest in the emission at the highest energies, we then examine the emission above 2.5 TeV with specially developed cuts.

## 2. Dataset

The detection of H1426+428 (H1426 in the following) as presented in Horan et al. (2002) is based on four separate datasets from 1995-98, 1999, 2000 and 2001 respectively. Since the sensitivity of the Whipple telescope was considerably improved over from 1995 to

Table 1: General properties of the H1426 dataset and the corresponding OFF dataset.

	ON	OFF
first MJD	51940	51875
last MJD	52275	52275
raw number of events	3698176	3826088
min. zenith angle	10°	6°
max. zenith angle	38°	38°
mean zenith angle	18.0°	18.7°
total observation time	38.1 h	39.9 h

2001 and the largest fraction of the observation time was invested in 2001, it was only in the 2001 dataset that a  $\gamma$ -ray signal with significance  $> 5\sigma$  was found. For this observing period, contemporaneous observations of the Crab Nebula are available (Krennrich et al. 2001) containing high-significance  $\gamma$ -ray signals which can serve to calibrate the telescope. In order to derive a spectrum for H1426, we have therefore chosen to confine ourselves to the 2001 dataset.

The dataset used here consists of 87 pairs of on-source (ON) and off-source (OFF) observations (“runs”). The run duration for the ON data varied between 10 and 28 minutes resulting in a total exposure time of 38.1 hours. The OFF dataset serves to determine the background caused by hadronic cosmic rays. Out of the 87 ON-OFF pairs in our dataset, 34 were taken in actual ON-OFF mode, i.e. with exactly matching zenith angle distribution and night sky background conditions. The OFF data for the remaining 46 ON runs was obtained by selecting matching OFF runs out of the pool of other OFF data taken in early 2001. The matching was based on how close to each other the runs were in terms of date, weather conditions, elevation and night sky brightness. This procedure results in a good agreement of the zenith angle distribution, but small discrepancies remain. Also, some of the OFF runs have a longer duration than their ON partners. As a result, the total OFF exposure time is 4.7 % longer than the ON exposure time. These differences were eliminated in later stages of the analysis by using the number of events not coming from the source direction to scale the background rate. This scaled background should be equal for both the ON and the OFF data.

### 3. Data analysis

#### 3.1. Determination of image parameters

The determination of the image parameters WIDTH, LENGTH, ALPHA, SIZE etc. for ON and OFF data was carried out following the standard procedure described in Reynolds et al. (1993) and Cawley (1993).

#### 3.2. Monte Carlo simulation

Our data was taken between  $10^\circ$  and  $38^\circ$  zenith angle with less than 10% taken at zenith angles between  $30^\circ$  and  $38^\circ$ . The average zenith angle is near  $20^\circ$ . The properties of air showers change as a function of the cosine of the zenith angle. Given the relatively large statistical error of the gamma signal from H1426 (see below), adequate accuracy for the determination of the detector sensitivity can therefore already be reached by simulating air showers only at the average zenith angle.

The shower simulation code ISUSIM (based on “cascade” by Kertzman & Sembroski (1994), see Mohanty et al. (1998)) was used to generate  $3.8 \times 10^6$  showers at zenith angle  $20^\circ$  between 0.05 TeV and 100 TeV with a spectral index of 2.5 (MC set 1). Other spectral indices were simulated by re-weighting. The simulation of the Whipple telescope was carried out with the “simveritas” code (Duke & LeBohec 2002, VERITAS internal report). The telescope parameters in this simulation were identical with those used in Krennrich et al. (2001).

#### 3.3. Derivation of the “Extended Cuts”

Using MC set 1 and the spectrum analysis algorithms developed in Mohanty et al. (1998), the “extended cuts” for the  $\gamma$ -hadron separation in our dataset were derived. These utilize only the image parameters WIDTH, LENGTH and ALPHA. They are derived as a second-order polynomial function of  $\log(\text{SIZE})$  by approximating the distributions of WIDTH and LENGTH and ALPHA as Gaussians and determining the mean  $a$  and the standard deviation  $\sigma$  as a function of  $\log(\text{SIZE})$ . The lower cuts on WIDTH and LENGTH respectively are then of the form  $(a - t\sigma)$  while the upper cuts are of the form  $(a + t\sigma)$ . The upper cut on ALPHA is also of the latter form. The constant  $t$ , the “tolerance”, determines the efficiency of the cuts. It is generally chosen to be 2.0 in order to minimize possible systematic effects arising from imperfections of the Monte Carlo simulations. In addition to the extended cuts, standard quality cuts were imposed as in

Krennrich et al. (2001).

#### 3.4. Background determination

Due to the 5% difference in exposure time and the remaining differences in elevation and night sky background, the number of events in the region  $\text{ALPHA} > 30^\circ$  (where according to simulations there should be no significant contribution caused by  $\gamma$ -rays from the source) is smaller for the ON data (184440 events) than it is for the OFF data (203531 events). The ratio  $r$  of these numbers (here 0.9062) can be used to scale the number of OFF events at small ALPHA in order to determine the background. Figure 2a shows the scaled OFF data distribution (with  $r = 0.9062$ ) superimposed on the ON distribution.

After applying the extended ALPHA cut (see Figure 1) the number of events is 51819 ON and 50279 OFF with an excess of 1540 events and significance  $5\sigma$ . Figure 2b shows that the shape of the ON and the OFF distributions agrees well in the normalization region ( $\text{ALPHA} > 30^\circ$ ).

#### 3.5. Energy reconstruction and binning

An algorithm described in Mohanty et al. (1998) was used to derive the coefficients in an analytical expression for the estimated primary  $\gamma$ -ray energy  $E_{\text{est}}$  from the Monte Carlo dataset 1 (see above). This expression is of the form

$$\log_{10}(E_{\text{est}}) = a_1 + a_2L + a_3D + a_4L^2 + a_5D^2 + a_6DL$$

where  $L = \log_{10}(\text{SIZE})$ ,  $D = \text{DIST}$ . This estimator gives a roughly constant energy resolution above 300 GeV. The energy resolution (the standard deviation in  $\log_{10}(E_{\text{est}})$ ) was determined near 400 GeV to be 0.166, i.e.  $\Delta E/E = 33\%$ . This value is used to determine the binning of the data with respect to  $\log_{10}(E_{\text{est}})$ . Statistics theory (Scott 1979) suggests that the ideal compromise between maximal structure resolution and minimal error in spectral parameters is achieved for weak signals if the energy bin width is chosen to be two standard deviations. In our case we must choose the energy bin width equal to  $2 \times 0.166 = 0.332$ .

The collection area of the telescope after our cuts on the image parameters reaches 10% of the maximum value (75,000 m<sup>2</sup>) at an energy of 250 GeV. The peak  $\gamma$ -rate for a standard spectrum of index 2.7 is observed near 410 GeV. We choose 250 GeV to be the lower edge of the second energy bin. The first energy bin will be excluded from fits of spectral functions. We

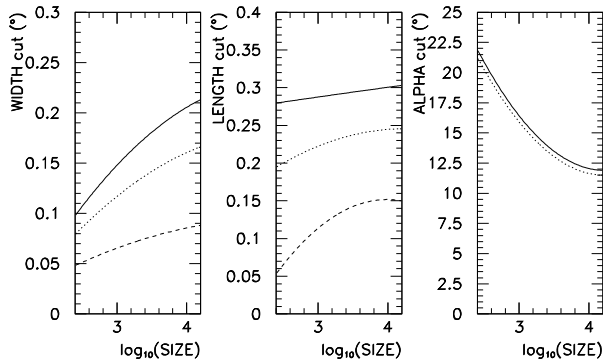


Fig. 1.— The upper (solid) and lower (dashed) “extended cuts” on the image parameters WIDTH, LENGTH and ALPHA as a function of  $\log(\text{SIZE})$  with tolerance  $t = 2.0$ . These cuts minimize systematic errors stemming from the simulations. The dotted lines show the upper cuts for maximum significance above 2.5 TeV (optimized on Crab Nebula data, see section 3.7).

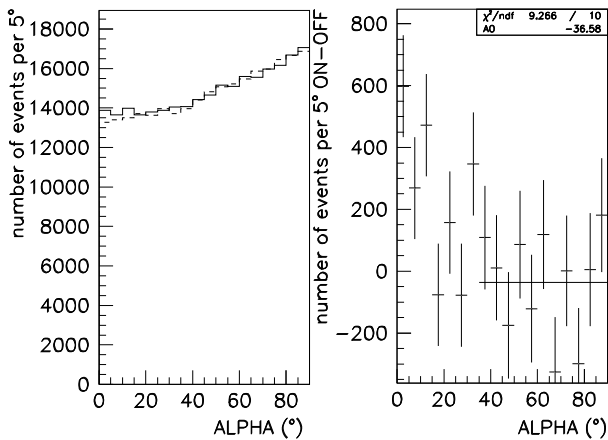


Fig. 2.— **(a)** (left) ALPHA distribution for the H1426 dataset ON (solid) and OFF (dashed, scaled by a factor 0.9062) after application of the extended cuts with  $t = 2.0$  described in section 3.3 except the cut on ALPHA. **(b)** (right) the difference between the two distributions shown in (a) with a constant function fitted to the region  $\text{ALPHA} > 30^\circ$ .

find this necessary since the systematic errors of the simulation at the trigger threshold are much larger than at higher energies. The first column of table 2 gives the logarithmic centers of the equidistant energy bins which result from these choices.

In order to ensure that the normalization constant  $r$  is independent of  $E_{\text{est}}$ , the ratio was measured separately in each energy bin. We find that the estimated energies in the H1426 ON dataset are systematically smaller than those in the OFF dataset by a small constant factor. By varying the factor until the scaling ratio  $r$  is the same within the statistical errors in all energy bins, we determine the value of  $K$ , the necessary correction factor for the estimated energies in the OFF data, to be  $K = 0.9784 \pm 0.005$ .

This small effect and its correction were studied in detail with datasets from observations of the Crab Nebula and Mkn 421 (two strong sources) and was found to be a result of the differences in the nightsky background conditions and zenith angle distributions. It was verified that the application of the correction factor  $K$  to the estimated energies of the OFF dataset results in correct spectral measurements. The statistical error of  $K$  leads to an increase of the statistical errors of the spectral parameters as discussed below.

### 3.6. Derivation of the H1426 spectrum

After application of the correction to the estimated energy and the scaling to the OFF data, we bin both ON and OFF events after all cuts in  $\log_{10}(E_{\text{est}})$ . For each of the energy bins, we determine a modified collection area  $A_\alpha$ . Its value depends on the assumed spectral index  $\alpha$  since the collection area has to be averaged over a finite energy bin width and the effects of the finite energy resolution will lead to spill-overs mostly from lower to higher bins, especially if the spectrum is steep. The differential flux in the energy bin  $i$  is then determined by

$$\left(\frac{dF}{dE}\right)_i = \frac{\text{ON}_i - \text{OFF}_i}{A_{\alpha,i} T \Delta E_i} \cdot k$$

where  $T$  is the observation time and  $\Delta E_i$  is the energy bin width. The factor  $k$  corrects for the approximate calculation of the energy derivative over a finite bin width. It has for our case the value 0.9313. Table 2 shows the event statistics for each energy bin.

Starting with the assumption that the spectral index will be similar to 2.5, we calculate the differential fluxes in each energy bin using  $A_{2.5}$  and fit a power

Table 2: The event statistics for the 2001 H1426+428 dataset after application of all extended cuts (tolerance  $t = 2.0$ ).

Energy (TeV)	ON (events)	OFF (events)	ON-OFF (events)	S ( $\sigma$ )
0.171	10341	10454	-113 $\pm$ 144	-0.78
0.369	23149	22255	894 $\pm$ 213	4.2
0.794	13887	13294	593 $\pm$ 164	3.6
1.71	3424	3283	141 $\pm$ 81	1.7
3.69	776	760	16 $\pm$ 39	0.41
7.94	209	200	9 $\pm$ 20	0.46
17.1	33	33	0 $\pm$ 8	0.0

law to the resulting values excluding the bin 1 with its large systematic errors. After iterating twice, using every time the spectral index  $\alpha$  resulting from the fit to recalculate  $A_\alpha$  and then recalculating the differential fluxes and repeating the fit, we reach convergence at  $\alpha = 3.50 \pm 0.30$ .

If we vary the correction  $K$  of the estimated energy for the OFF data within its statistical errors, we find that the resulting  $\alpha$  varies by  $\pm 0.18$ . This has to be regarded as an additional, to a good approximation uncorrelated, error since the uncertainty of  $K$  stems from a finite number of events which are different from those events used to measure  $\alpha$ . The total statistical error on  $\alpha$  is therefore  $\sqrt{0.30^2 + 0.18^2} = 0.35$ . The systematic error on  $\alpha$  for our method has to be determined from a dataset with small statistical errors. This was done in Krennrich et al. (2001). By varying the cut tolerance  $t$  between 1.5 and 3.0 on a Crab Nebula dataset, the systematic error was determined to be  $\pm 0.05$ .

The statistical error on the exponent of the flux constant is determined correspondingly  $\sqrt{0.11^2 + 0.10^2} = 0.15$  while the systematic error is derived by varying the absolute energy calibration by  $\pm 15\%$ . Note that the steepness of the spectrum makes this systematic error especially large. The final result is

$$\frac{dF}{dE} = 10^{-7.31 \pm 0.15_{\text{stat}} \pm 0.16_{\text{syst}}} \times E^{-3.50 \pm 0.35_{\text{stat}} \pm 0.05_{\text{syst}}} \text{ m}^{-2} \text{ s}^{-1} \text{ TeV}^{-1}$$

### 3.7. Evidence for emission above 2.5 TeV

The extended cuts are designed to minimize systematic errors of the flux measurement. When purely statistical evidence for the presence of emission is required, these cuts are inadequate for weak sources. This is the case for H1426 above 2.5 TeV, where the statistical sig-

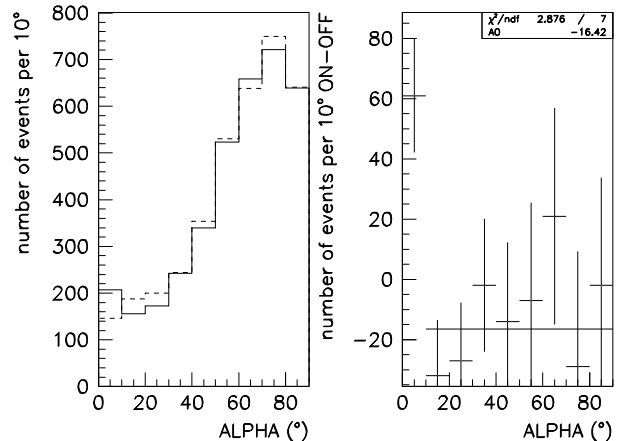


Fig. 3.— As Figure 2, but only showing events with estimated energy above 2.5 TeV and using tighter cuts optimized on Crab Nebula data to give maximum significance above 2.5 TeV. The excess is expected at  $\text{ALPHA} < 12^\circ$ .

nificance of the excess obtained with the extended cuts drops well below  $1 \sigma$  in each energy bin. The question whether emission is present above a few TeV is, however, so important for this source that a special effort is justified.

Using 15.1 hours of contemporaneous Crab Nebula observations and a matching OFF dataset, we optimize a set of cuts to give maximum significance above 2.5 TeV. With the standard extended cuts, the significance is  $5.5\sigma$ . In the optimization, we vary independently the tolerance  $t$  for the upper cuts on WIDTH, LENGTH and ALPHA keeping the tolerance for the lower cuts on WIDTH and LENGTH constant at 2.0. In addition we require that at least 70 % of the excess obtained with the standard extended cuts is retained. The maximum significance ( $8.3\sigma$ ) for the excess above an estimated energy of 2.5 TeV is reached for tolerance  $t = 0.5$  for the upper WIDTH and LENGTH cuts and  $t = 1.9$  for the ALPHA cut. These cuts are shown as dotted lines in Figure 1.

When applied to the H1426 dataset (using a recalculated energy estimation and correction  $K$ , see above), the optimized cuts improve the significance above 2.5 TeV as one would expect in the case that emission is actually present. Taking into account the error of the correction factor  $K$  for the estimated energy of the background events, there are  $59 \pm 22.7$  excess events with estimated energy above 2.5 TeV. This corresponds to

( $12 \pm 5$ )% of the excess rate observed from the Crab Nebula. The statistical evidence for emission from H1426 above 2.5 TeV is  $2.6 \sigma$ . Figure 3 shows the ALPHA distribution of the H1426 events with estimated energy above 2.5 TeV after the optimized cuts.

#### 4. Discussion

The spectral index found in this analysis agrees well with the first result ( $\alpha = 3.55 \pm 0.5$ ) published in Horan et al. (2002). The flux normalization constant is larger than that in Horan et al. (2002) but well within the statistical and systematic errors of this result which was obtained using a different analysis method and different Monte Carlo data.

The only other published detection of H1426+428 at  $\gamma$ -ray energies comes from HEGRA (Aharonian et al. 2002) and is based on a dataset of similar size. The two results are compared in the following.

From a total of 44.4 hours HEGRA obtains a total number of excess events of 199.2 after loose cuts for their spectral analysis. The significance is  $4.3 \sigma$ . We obtain a slightly higher significance and an excess of 1540 events from 38.1 hours of data using similarly loose cuts. The relative numbers of events recorded by HEGRA and Whipple are consistent with the difference in energy threshold which is a factor of  $\approx 2.5$ . An estimation of the integral spectral index from these numbers gives a value of 2.2 which already hints that the spectrum must be steep if there was no significant change in the overall state of the source between 1999/2000 and 2001.

Direct comparison of the individual spectral points (Figure 4) shows a very good agreement indicating that there really was little change in the overall state of the source between the observing periods. Given the 30% systematic errors of the absolute flux calibration of both our and the HEGRA measurement, this is consistent with the fact that the  $\gamma$ -ray rates measured by Horan et al. (2002) for the 2000 and the 2001 H1426 dataset differ only by a factor 1.5.

To make use of the total available information, we perform a fit of a power-law to the combined points from HEGRA and our analysis. No adjustments to the overall normalization of any of the datasets was performed since the points near 790 GeV agree very well. The errors on the Whipple points included in this fit take into account both the Gaussian error of the number of excess events ( $\sqrt{N_{\text{on}} + N_{\text{off}}}$ ) and the uncertainty stemming from the energy estimation for the

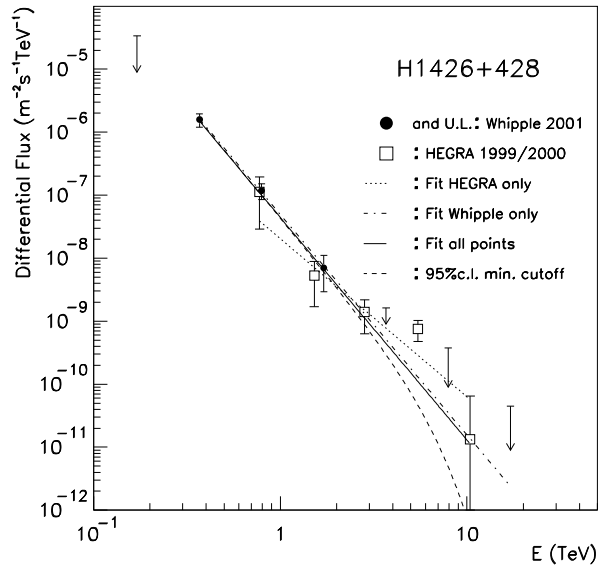


Fig. 4.— The differential energy spectrum of H1426+428 as measured in this analysis (filled points and upper limits) in 2001 and by HEGRA (open squares) in 1999/2000 (Aharonian et al. 2002). The 84% confidence level upper limits were obtained using the method by Helene (1983). The solid line is the result of a power law fit to all points except the upper limit at the lowest energy. The dashed line shows the scenario of the latter power law with an additional abrupt (super-exponential) cutoff still consistent with all data at the 95% confidence level. The minimum cutoff energy found for this scenario is 6 TeV. Also shown is the power-law fit to the HEGRA points only (dotted) and the power-law fit to the Whipple points only (dot-dashed).

background. The fit to all points (still excluding the upper limit at the lowest energies) results in a spectrum which is essentially identical with what we obtain from our points only. However, the statistical errors are smaller:

$$\frac{dF}{dE} = 10^{-7.36 \pm 0.07_{\text{stat}}} \cdot E^{-3.54 \pm 0.27_{\text{stat}}} \text{ m}^{-2} \text{ s}^{-1} \text{ TeV}^{-1}$$

The reduced  $\chi^2$  of this fit to 11 points is 0.94. The measurements are consistent with the assumption that the spectrum of H1426 is a continuous powerlaw between 250 GeV and 17 TeV.

In order to further quantify the evidence for high-energy emission, we introduce a super-exponential cutoff in the measured power-law. This cutoff can be described analytically ( $\exp(-(E/E_0)^2)$ ) and is reasonably abrupt such that it can serve as a parameter describing the energy above which there is no emission from the source. By keeping the nominal values of the power-law fit for normalization and spectral index and reducing the cutoff energy  $E_0$  until the  $\chi^2$  of a fit to all significant points (i.e. excluding the points shown in Figure 4 as upper limits) has increased to 14.1 (95% confidence level for 7 degrees of freedom) we obtain  $E_0 = 5.5$  TeV.

Independently, we verify if this value for  $E_0$  is consistent with the fact that we observe from H1426  $12 \pm 5\%$  of the Crab Nebula  $\gamma$ -rate above 2.5 TeV (see section 3.7). Taking into account the larger spill-over effects caused by the finite energy resolution of our instrument and the steep spectrum of H1426 and furthermore the 15% uncertainty of our absolute energy calibration, we find that a 95% confidence level lower limit on the integral flux of H1426 above 2.5 TeV can be put at 3% of the Crab Nebula flux. Using our measurement of the Crab Nebula flux with the same instrument, this corresponds to

$$F_{\text{H1426}}(E > 2.5 \text{ TeV}) > 1.06 \times 10^{-9} \text{ m}^{-2} \text{ s}^{-1} \quad (95\% \text{ c.l.})$$

Varying the cutoff energy  $E_0$  introduced above until the integral flux above 2.5 TeV has the value of this lower limit, we find a value of  $E_0 = 6$  TeV which independently confirms the result from above. The spectrum with  $E_0 = 6$  TeV is shown as a dashed line in Figure 4.

The HEGRA collaboration attempts to reconstruct the intrinsic energy spectrum of the source by assuming a model for the intergalactic IR background and calculating the expected absorption for  $\gamma$ -rays coming from H1426 (redshift 0.129). They arrive at an intrinsic spectrum with index 1.9 and find that the ‘‘upturn’’ in the spectrum around a few TeV may be explained

by a decrease of the slope of the  $\gamma$ -ray absorption as a function of energy. Our data is not inconsistent with the absorbed spectrum derived by HEGRA. In fact, our lowest point at 370 GeV agrees very well with the hypothesis of the absorbed spectrum, but not with the extrapolation of the alternatively fitted power law (dotted line in Figure 4). The latter can be excluded with a confidence level  $> 99.5\%$  which argues for a flattening of the spectrum at a few TeV. More data is needed to confirm this result.

Between 250 GeV and 800 GeV, our data clearly favours a spectrum which is steeper than that of any other known TeV blazar at these energies. Since H1426 is also the most distant known TeV blazar, the steepness of the spectrum may be interpreted as evidence for gamma-ray absorption in the intergalactic medium. However, the sample of TeV blazars still needs to be enlarged and the intrinsic spectrum well separated from absorption effects before one can come to firm conclusions.

The VERITAS Collaboration is supported by the U.S. Department of Energy, National Science Foundation, the Smithsonian Institution, P.P.A.R.C. (U.K.) and Enterprise Ireland.

## REFERENCES

- Aharonian, F., et al. 2002, *A&A*, 384, L23
- Cawley, M.F. 1993, in ‘‘Towards a major atmospheric Cherenkov detector II (Calgary)’’, ed. R.C. Lamb, 176
- Costamante, L., et al. 2001, *A&A*, 371, 512
- Costamante, L. & Ghisellini, G. 2002, *A&A*, 384, 56
- Donato, D., et al. 2001, *A&A*, 375, 739
- Ghisellini, G. 2000, in *ASP Conf. Ser.*, X-ray Astronomy 2000, ed. R. Giacconi et al., 234 (*astro-ph/0012125*)
- Helene, O. 1983, *NIM*, 212, 319
- Horan, D., et al. 2002, *ApJ*, 571, 753
- Kertzman, M.P. & Sembroski, G.H. 1994, *NIM A*, 343, 629
- Krennrich, F., et al. 2001, *ApJ*, 560, L45
- Mohanty, G., et al. 1998, *Astropart. Phys.*, 9, 15

Rachen, J.P. 2000, in AIP Conf. Proc. 558, High Energy Gamma-Ray Astronomy, ed. F.A. Aharonian & H.J. Völk, 704 (astro-ph/0010289)

Reynolds, P.T., et al. 1993, ApJ 404, 206

Remillard, R.A., et al. 1989, ApJ, 345, 140

Scott, D.W. 1979, Biometrika, 66, 605

Sikora, M. & Madejski, G. 2000, in AIP Conf. Proc. 558, High Energy Gamma-Ray Astronomy, ed. F.A. Aharonian & H.J. Völk, 275 (astro-ph/0101382)